Ceramide is a cardiotoxin in lipotoxic cardiomyopathy[s]

Tae-Sik Park,[*,§] Yunying Hu,[*] Hye-Lim Noh,[*] Konstantinos Drosatos,[*] Kazue Okajima,[†] Jonathan Buchanan,[**] Joseph Tuinei,[**] Shunichi Homma,[†] Xian-Cheng Jiang,[††] E. Dale Abel,[**] and Ira J. Goldberg[1,*]

Divisions of Preventive Medicine and Nutrition,[*] and Cardiology,[†] Department of Medicine, Columbia University, College of Physicians and Surgeons, New York, NY 10032; Lee Gil Ya Cancer and Diabetes Institute,[§] Gachon University of Medicine and Science, Inchon, South Korea; Program in Human Molecular Biology and Genetics and Division of Endocrinology, Metabolism, and Diabetes,[**] University of Utah School of Medicine, Salt Lake City, UT 84112; and Department of Anatomy and Cell Biology,[††] SUNY Downstate Medical Center, Brooklyn, NY 11203

Abstract Ceramide is among a number of potential lipotoxic molecules that are thought to modulate cellular energy metabolism. The heart is one of the tissues thought to become dysfunctional due to excess lipid accumulation. Dilated lipotoxic cardiomyopathy, thought to be the result of diabetes and severe obesity, has been modeled in several genetically altered mice, including animals with cardiac-specific overexpression of glycosylphosphatidylinositol (GPI)-anchored human lipoprotein lipase (LpL[GPI]). To test whether excess ceramide was implicated in cardiac lipotoxicity, de novo ceramide biosynthesis was inhibited pharmacologically by myriocin and genetically by heterozygous deletion of LCB1, a subunit of serine palmitoyltransferase (SPT). Inhibition of SPT, a rate-limiting enzyme in ceramide biosynthesis, reduced fatty acid and increased glucose oxidation in isolated perfused LpL[GPI] hearts, improved systolic function, and prolonged survival rates.▪ Our results suggest a critical role for ceramide accumulation in the pathogenesis of lipotoxic cardiomyopathy.—Park, T.-S., Y. Hu, H-L. Noh, K. Drosatos, K. Okajima, J. Buchanan, J. Tuinei, S. Homma, X-C. Jiang, E. D. Abel, and I. J. Goldberg. **Ceramide is a cardiotoxin in lipotoxic cardiomyopathy.** *J. Lipid Res.* 2008. **49: 2101–2112.**

Supplementary key words serine palmitoyltransferase • lipotoxicity • heart • glucose • fatty acid

Increasing caloric intake and greater body mass index produce a series of diseases due to tissue lipid accumulation. As storage capacity of adipocytes is exceeded, fat begins to infiltrate the liver, skeletal muscle, and heart (1, 2). In addition to triglyceride (TG), these tissues also have increased levels of FAs, fatty acyl CoA, diacylglycerol (DAG), and ceramide (3, 4).

Cardiac ceramide levels are elevated in models of cardiac lipotoxicity due to cardiac overexpression of long-chain acyl CoA synthase (5), PPARα (6), PPARγ (7), and FATP (8). Ceramide is produced by two pathways: *1)* condensation of palmitoyl CoA with serine by serine palmitoyltransferase (SPT) (9), and *2)* sphingomyelinase hydrolysis of sphingomyelin (SM) (10). Recently, Holland et al. (4) compared the effects of soybean- and lard-based emulsion infusions and suggested that the two types of lipids cause insulin resistance via different mechanisms. Only saturated fat increased tissue ceramide levels. Genetic and pharmacologic inhibition of the de novo ceramide biosynthetic pathway ameliorated insulin resistance.

Aside from ceramide, DAG and/or FA could be responsible for dilated lipotoxic cardiomyopathy. DAG activates protein kinase C in skeletal muscle and aorta, which is associated with insulin resistance (11–13). Excess FAs, especially saturated FA, increase reactive oxygen species (ROS) formation (14), create endoplasmic reticulum stress, and activate apoptotic pathways in several cell lines, including adipocytes and cardiomyocytes (15–17). In addition, high plasma FAs created by infusion of soybean lipid emulsions and heparin into animals activate toll-like receptors and NFκB (18).

We have previously studied mice with cardiomyocyte overexpression of a glycosylphosphatidylinositol (GPI) membrane-anchored form of lipoprotein lipase, denoted LpL[GPI], that develop dilated cardiomyopathy (19). These hearts have an accumulation of ceramide. In this report, we show that ceramide accumulation plays a significant role

---

Abbreviations: DAG, diacylglycerol; 2-DG, 2-deoxy-D-glucose; GPI, glycosylphosphatidylinositol; LCB1^{+/−}, heterozygous LCB1 knockout; LVD, left ventricular systolic diameter; LpL, lipoprotein lipase; ROS, reactive oxygen species; SM, sphingomyelin; SPT, serine palmitoyltransferase; TG, triglyceride; WT, wild type.

[1] To whom correspondence should be addressed.
   e-mail: ijg3@columbia.edu
[s] The online version of this article (available at http://www.jlr.org) contains supplementary data in the form of two figures and one table.

in the progression of the dilated cardiomyopathy seen in LpL^{GPI} mice. Using pharmacologic and genetic methods, we tested whether inhibition of SPT in normal and lipotoxic hearts altered cardiac ceramide concentrations and cardiac substrate utilization. Reduction of ceramide was associated with improved cardiac function, reversal of abnormal substrate use, and improved survival.

MATERIALS AND METHODS

Myriocin treatment of transgenic mice

Generation of LpL^{GPI} transgenic mice has been described previously (19). LpL^{GPI} and wild-type (WT) C57BL/6J mice (8–10 weeks old) were fed either a chow diet (Research Diets, New Brunswick, NJ) or chow mixed with myriocin (Sigma Adrich, St. Louis, MO, prepared by Research Diets) (0.3 mg/kg/day) for 6 weeks. Heterozygous LCB1 knockout (LCB1$^{+/-}$) and LCB1$^{+/-}$ crossed with LpL^{GPI} transgenic mice were fed a normal chow diet. For survival analyses, the same dose of myriocin was fed to 12 week-old LpL^{GPI} (n = 14) and C57Bl/6J mice (n = 14) for 40 weeks. All animals were maintained on a 12 h light-dark cycle.

AC16 cardiomyocytes

Generation of a human cardiomyocyte cell line, AC16, has been described previously by Davidson et al. (20). Cells were grown in DMEM/F12 media containing 12.5% FBS and incubated at 37°C in an atmosphere containing 5% CO_2/95% air. Cardiomyocytes that were 70–80% confluent were switched to DMEM/F12 media containing 1% FBS and treated with various concentrations of palmitic acid conjugated with 2% FA-free BSA in the presence or absence of 1 µM myriocin for 16 h. In other experiments, cells were treated with C6-ceramide for 16 h after incubation in DMEM/F12 containing 2% FA-free BSA. mRNA for RT-PCR was isolated using TRizol (Invitrogen).

Substrate metabolism in isolated working mouse hearts

Cardiac metabolism was measured in hearts isolated from 14 to 16 week-old male WT and LpL^{GPI} mice (n = 5 per genotype). All hearts were prepared and perfused in the working mode, using protocols that have been previously described (21–24).

Heart and plasma lipids

Heart lipids were extracted as described by Folch, Lees, and Sloane Stanley (25). TG and cholesterol concentrations in hearts and plasma were measured using TG and cholesterol enzymatic assay kits (Infinity, Louisville, CO); FFAs were measured using NEFA C kits (Wako Chemicals, Richmond, VA). Tissue lipids were normalized by protein concentration. Cardiac and plasma SM levels were measured enzymatically as described previously (26). Cardiac ceramide and DAG levels were determined using the DAG kinase method (27). Cardiac acyl CoAs were measured by liquid chromatography/tandem mass spectrometry using Perkin Elmer S200 HPLC (Perkin Elmer, Waltham, MA) and API 3000 (Applied Biosystems, Foster City, CA) and analyzed by Analyst 1.4.1 software (Applied Biosystems).

Echocardiography

Two-dimensional echocardiography was performed on conscious 14 to 16 week-old male (n = 10–12 per group) mice (Sonos 5500 system; Philips Medical Systems, Andover, MA) (28). Echocardiographic images were recorded in a digital format. Images were then analyzed off-line by a single observer blinded to the murine genotype (29).

Gene expression

Quantitative real-time PCR was performed with SYBR Green PCR Core Reagents (Applied Biosystems). Incorporation of the SYBR green dye into the PCR products was monitored in real time with an Mx3000 sequence detection system (Stratagene, La Jolla, CA). Samples were normalized against β-actin. The sequences of the primers are provided in supplementary Table I.

Western blots

Isolated heart tissues were homogenized in PBS containing protease inhibitors and phosphatase inhibitors (Roche, Indianapolis, IN). Membrane and cytosolic fractions were separated by ultracentrifugation. Thirty micrograms from each fraction was applied to SDS-PAGE and transferred onto nitrocellulose membranes. GLUT4 and GLUT1 proteins in each fraction were detected by mouse-specific antibodies (Chemicon, Temecula, CA). Thirty micrograms of whole-tissue extracts was applied for Western blot analyses to examine phosphorylated (p) GSK-3β and pAKT, which were detected by mouse-specific antibodies (Cell Signaling, Danvers, MA).

Glucose uptake studies

Basal glucose uptake was measured in hearts following an intravenous administration of 3 µCi of 2-deoxy-D-[1-^{14}C]glucose (Perkin-Elmer Life Sciences). Blood was collected 30 s and 5, 30, and 60 min following injection. At 60 min, hearts were perfused with PBS, tissues were excised, and radioactive counts were measured.

Histology

Hearts from 6 h-fasted mice were fixed in 10% formalin for 24 h and mounted on paraffin. Midventricular sections were stained with Schiff Reagent (Polyscientific, Bay Shore, NY) to identify glycogen in hearts [periodic acid-Schiff (PAS) staining] (30). The specificity of glycogen staining was confirmed by treating sections with diastase to digest tissue glycogen, followed by regular PAS staining (30). Sectioned heart tissues were stained for DNA fragmentation by a terminal deoxynucleotidyl transferase-mediated dUTP-biotin nick end labeling (TUNEL) staining protocol according to the manufacturer's instructions (R and D Systems, Minneapolis, MN).

Glycogen analysis

Hearts were hydrolyzed with 1 M NaOH at 65°C for 2 h, and glycogen was precipitated by 66% cold ethanol. Cardiac glycogen was digested by amyloglucosidase at 45°C for 2 h (31). The produced glucose was measured enzymatically by an AutoGlucose kit (Wako Chemicals).

Statistics

Cardiac metabolism data in isolated working hearts were analyzed by ANOVA, and significance was evaluated by the Fisher Least Protected Squares test. Differences among groups were determined using one-way ANOVA with post hoc Dunnett's t-test. A value of $P < 0.05$ was regarded as a significant difference.

RESULTS

Myriocin lowers sphingolipids in plasma and heart

During myriocin treatment for 6 weeks, no significant changes in body weight, plasma glucose, cholesterol, TG, and FFA levels were observed (**Table 1**). Myriocin lowered plasma SM levels significantly in WT and LpL^{GPI} mice.

TABLE 1. Body and heart weight, glucose, and plasma lipid measurements in WT and LpL^{GPI} mice

	WT	WT-myr	LpL^{GPI}	LpL^{GPI}-myr
Body wt. (g)	29.8 ± 2.1	27.7 ± 1.5	29.5 ± 1.5	30.6 ± 3.5
Heart wt./body wt. (%)	0.58 ± 0.02	0.53 ± 0.06	0.64 ± 0.02[a]	0.51 ± 0.02[a,b]
Glucose (mg/dl)	108 ± 3.9	103 ± 6.0	102 ± 7.7	104 ± 6.4
TG (mg/dl)	70.5 ± 12.7	63.9 ± 4.8	78.0 ± 9.5	73.5 ± 2.4
Cholesterol (mg/dl)	69.1 ± 1.75	74.5 ± 3.4	64.4 ± 4.7	74.1 ± 5.5
FFA (mM)	0.61 ± 0.12	0.44 ± 0.13	0.51 ± 0.08	0.43 ± 0.05
SM (μg/ml)	24.9 ± 2.3	12.1 ± 1.6[a]	21.1 ± 5.0	9.1 ± 2.0[a,b]

LpL^{GPI}, glycosylphosphatidylinositol (GPI)-anchored human lipoprotein lipase; SM, sphingomyelin; myr, myriocin; TG, triglyceride; WT, wild type. Results are given as mean ± SEM, n = 8–10.

[a] $P < 0.05$ (vs. WT).
[b] $P < 0.05$ (vs. LpL^{GPI}).

TG and cholesterol levels in mouse hearts were not changed by myriocin treatment or overexpression of LpL (**Table 2**). SM levels were 45% less in hearts of myriocin-treated LpL^{GPI} than in untreated mice of the same genotype. In contrast, SM levels were not altered in WT mice (Table 2). Cardiac ceramide levels were increased approximately 45% in LpL^{GPI} mouse hearts. Treatment with myriocin reduced ceramide to control levels (Table 2). Myriocin-treated WT mice did not show alteration of cardiac ceramide. This appeared to be due to upregulation of SPT subunits LCB1 and LCB2 as a compensatory mechanism to maintain basal sphingolipid pools (**Table 3**). DAG was also elevated in LpL^{GPI} hearts, but myriocin had no effect on cardiac DAG levels (Table 2). Acyl CoAs were reduced in LpL^{GPI} hearts, and myriocin treatment restored them to WT levels (Table 2). Thus, myriocin lowered cardiac SM and ceramide without changing TG, cholesterol, and DAG levels. Moreover, the improved hearts had a normalization of the reduced acyl CoA. We assumed that this was a secondary change due to reduced FA oxidation (see below).

Myriocin improves cardiac function in LpL^{GPI} mice and reduces expression of heart failure markers

LpL^{GPI} hearts were hypertrophied with an increase in heart/body weight (Table 1; **Fig. 1A**). Myriocin treatment of these mice returned heart weights to WT levels. Echocardiography also revealed that hearts from chow-fed LpL^{GPI} mice had left ventricular dilatation, increased left ventricular systolic diameter (LVD), and decreased fractional shortening, compared with hearts from chow-fed WT mice, as previously reported (19). The LVDs of myriocin-treated LpL^{GPI} mice were comparable to those of WT mice and were smaller than those of untreated LpL^{GPI} mice (0.18 ± 0.014 cm vs. 0.24 ± 0.014 cm) (Fig. 1B). Reduced fractional shortening in LpL^{GPI} mice was corrected by myriocin (46.1 ± 2.0% in myriocin-LpL^{GPI} vs. 35.5 ± 2.0% in LpL^{GPI} mice) (Fig. 1C).

We assessed whether myriocin affected markers of cardiac failure. ANF and BNP gene expression was increased in LpL^{GPI} hearts when compared with WT, and myriocin treatment reduced mRNA levels of these genes even further than those of WT (Table 3). Thus, treatment with myriocin that specifically reduced cardiac ceramide and had no impact on the levels of other major lipids improved cardiac function and reduced gene expression of cardiac failure markers.

Effects of myriocin on cardiac gene expression

We assessed whether myriocin affected expression of metabolic genes in WT and LpL^{GPI} hearts. GLUT4 was downregulated in LpL^{GPI} hearts, and myriocin had no effect (Fig. 1D). GLUT1 expression was not altered by LpL overexpression or myriocin treatment (Fig. 1E). PDK4 mRNA was increased in hearts of LpL^{GPI} mice (Fig. 1F). Increased PDK4 increases phosphorylation of pyruvate dehydrogenase and would be expected to reduce glucose oxidation rates in isolated hearts. Myriocin restored upregulation of PDK4 in LpL^{GPI} hearts to WT levels. Expression levels of genes that regulate FA oxidation, such as PPAR-α, CPT-1, and ACO, were not changed in LpL^{GPI} hearts by myriocin treatment (see supplementary Fig. I). Expression of fatty acid transporters such as CD36, acyl CoA synthase1 (ACS1), and fatty acid transport protein1 (FATP1) were

TABLE 2. Cardiac lipid measurement in WT and LpL^{GPI} mice

	WT	WT-myr	LpL^{GPI}	LpL^{GPI}-myr
TG (μg/mg)	16.8 ± 6.5	19.1 ± 9.0	18.1 ± 9.5	22.2 ± 8.0
Cholesterol (μg/mg)	4.2 ± 1.0	4.2 ± 0.18	5.0 ± 1.0	5.3 ± 0.7
Fatty acyl CoA (pmol/mg)	81.4 ± 6.2	130.6 ± 4.8[a]	41.4 ± 11.2[a]	122.1 ± 4.8[a,b]
SM (μg/mg)	15.2 ± 2.5	14.6 ± 2.1	22.2 ± 1.9[a]	12.2 ± 2.3[a,b]
Ceramide (pmol/mg)	210.5 ± 11.3	216.3 ± 22.6	305.9 ± 21.1[a]	151.8 ± 9.9[a,b]
DAG (pmol/mg)	184.4 ± 4.9	176.4 ± 8.5	233.5 ± 5.6[a]	228.0 ± 8.7[a]

DAG, diacylglycerol. Results are given as mean ± SEM, n = 8–10.

[a] $P < 0.05$ (vs. WT).
[b] $P < 0.05$ (vs. LpL^{GPI}).

TABLE 3. Expression of SPT subunits and heart failure markers in WT and LpL[GPI] mice

Gene	4 month-old			
	WT	WT-myr	LpL[GPI]	LpL[GPI]-myr
LCB1	1.00 ± 0.14	2.19 ± 0.19[a]	0.61 ± 0.05[a]	1.19 ± 0.19[b]
LCB2	1.00 ± 0.14	2.32 ± 0.38[a]	0.87 ± 0.04	1.61 ± 0.22[b]
ANF	1.00 ± 0.09	0.81 ± 0.22	1.74 ± 0.20[a]	0.47 ± 0.15[a,b]
BNP	1.00 ± 0.22	1.14 ± 0.17	2.27 ± 0.45[a]	0.51 ± 0.12[a,b]

SPT, serine palmitoyltransferase. Results are given as mean ± SEM, n = 8–10.
[a] $P < 0.05$ (vs. WT).
[b] $P < 0.05$ (vs. LpL[GPI]).

downregulated in LpL[GPI] hearts (Fig. 1G, H, I). Myriocin restored them to the levels of WT.

Myriocin corrects the increased FA and reduced glucose oxidation in LpL[GPI] hearts

Cardiac metabolism was measured in hearts from 14 to 16 week-old male WT and LpL[GPI] mice. All hearts were prepared and perfused in the working mode, using previously described protocols (21–24). Palmitate oxidation was increased by 27% and glucose oxidation was decreased by 26% in LpL[GPI] hearts relative to controls (**Fig. 2A, B**). Myriocin treatment reduced palmitate oxidation and increased glucose oxidation rates in LpL[GPI] hearts to the levels of WT (Fig. 2A, B). The average rates of glycolysis were not altered (Fig. 2C). Thus, hearts of LpL[GPI] mice develop altered substrate utilization with increased reliance on FAs, and myriocin altered substrate utilization by reducing FA oxidation and increasing glucose oxidation in LpL[GPI] hearts. In isolated working hearts, we did not detect any improvement in cardiac power following treatment of LpL[GPI] mice with myriocin (Fig. 2D). However, there was a significant reduction in MVO₂ (Fig. 2E). This normalized cardiac efficiency (Fig. 2F), which was reduced in hearts from nontreated mice. These data suggest that myriocin enhanced myocardial energetics by maintaining cardiac performance at a lower oxygen cost. The gene expression data suggest that the increase in oxidation rates of exogenous palmitate in LpL[GPI] hearts might be the consequence of the PDK4-mediated reduction in pyruvate flux, which would reduce glucose oxidation.

In vivo uptake of glucose in WT and myriocin-treated LpL[GPI] hearts

We examined whether in vivo glucose uptake was affected by myriocin using 2-deoxy-D-[1-^{3}H]glucose (2-DG). There was no difference in plasma glucose clearance between WT and LpL[GPI] mice (**Fig. 3A**). In contrast to findings in isolated hearts (reduced glucose oxidation and normal rates of glycolysis), in vivo glucose uptake was increased in LpL[GPI] mouse hearts (Fig. 3B). Myriocin reduced in vivo glucose uptake in LpL[GPI] hearts to the levels of WT. The estimation of glycolytic rates in isolated hearts is based on the appearance of ^{3}H, which is released as water at the final step in glycolysis, whereas 2-DG measures glucose transport and phosphorylation. If exogenous glucose uptake is increased but the glucose is not being oxidized,

more glucose might be converted to glycogen; this would account for the differences between measurements obtained in vivo versus those obtained in isolated hearts.

Histological analysis of heart tissue by PAS staining demonstrated that hearts of LpL[GPI] mice had greater glycogen stores than did hearts of myriocin-treated WT and LpL[GPI] mice (Fig. 3C). In contrast, hearts of LpL[GPI] mice treated with myriocin had a pattern of glycogen staining that was similar to that of WT mouse hearts (Fig. 3C). To confirm this, we biochemically measured cardiac glycogen. Glycogen content in hearts of LpL[GPI] mice was 49% greater than that in hearts of WT mice (Fig. 3D). Hearts of myriocin-treated LpL[GPI] mice had glycogen levels similar to those in hearts of WT mice (Fig. 3D). Thus, in hearts of LpL[GPI] mice, glucose carbons appear to preferentially accumulate as glycogen; myriocin treatment reversed this process.

Phosphorylation of AKT and GSK-3β

To assess whether the AKT/GSK-3β pathway was involved in hypertrophy and glycogen synthesis in hearts of LpL[GPI] mice, pAKT and its downstream target, pGSK-3β, were examined by Western blot. PAKT and pGSK-3β were elevated in hearts of LpL[GPI] mice, compared with hearts of WT mice (Fig. 3E–G). Myriocin treatment decreased pAKT and pGSK-3β levels in hearts of LpL[GPI] mice by 63% and 53%, respectively (Fig. 3E–G). GSK-3β blocks cardiac hypertrophy and inhibits glycogen synthesis. GSK-3β inactivation by phosphorylation would be predicted to promote cardiac hypertrophy and increase glycogen synthesis in the hearts of LpL[GPI] mice.

Effects of ceramide on the expression of glucose-metabolizing genes and cardiac failure markers in AC16 human cardiomyocytes

Using recently developed human cardiomyocyte AC16 cells (20), we tried to reproduce conditions associated with lipotoxic cardiomyopathy and then examine whether ceramide alters cardiac substrate utilization in a direct manner, as opposed to metabolic changes being secondary to cardiac dysfunction. To do this, we grew cells in the presence or absence of C6-ceramide and examined the gene expression. Ceramide downregulated GLUT4 expression and upregulated PDK4 (**Fig. 4A**). Ceramide also upregulated ANF and BNP (Fig. 4B). These changes in gene expression are consistent with the in vivo gene expression profile in LpL[GPI] mice with elevated cellular levels of ceramide. In contrast, C6-ceramide treatment of AC16 cardiomyocytes decreased pAKT and pGSK-3β in a concentration-dependent manner (Fig. 4C); these decreases were opposite to the in vivo results.

Myriocin decreases mortality rates in LpL[GPI] mice

Myriocin was administered to LpL[GPI] mice to assess whether improved cardiac function was associated with improved survival of this lipotoxic cardiomyopathic animal model. First, we sought to determine whether ceramide accumulation increased apoptosis in LpL[GPI] hearts and whether limiting apoptosis could account in part for the beneficial effect of myriocin. However, we did not detect any increase in TUNEL-positive staining in the hearts of
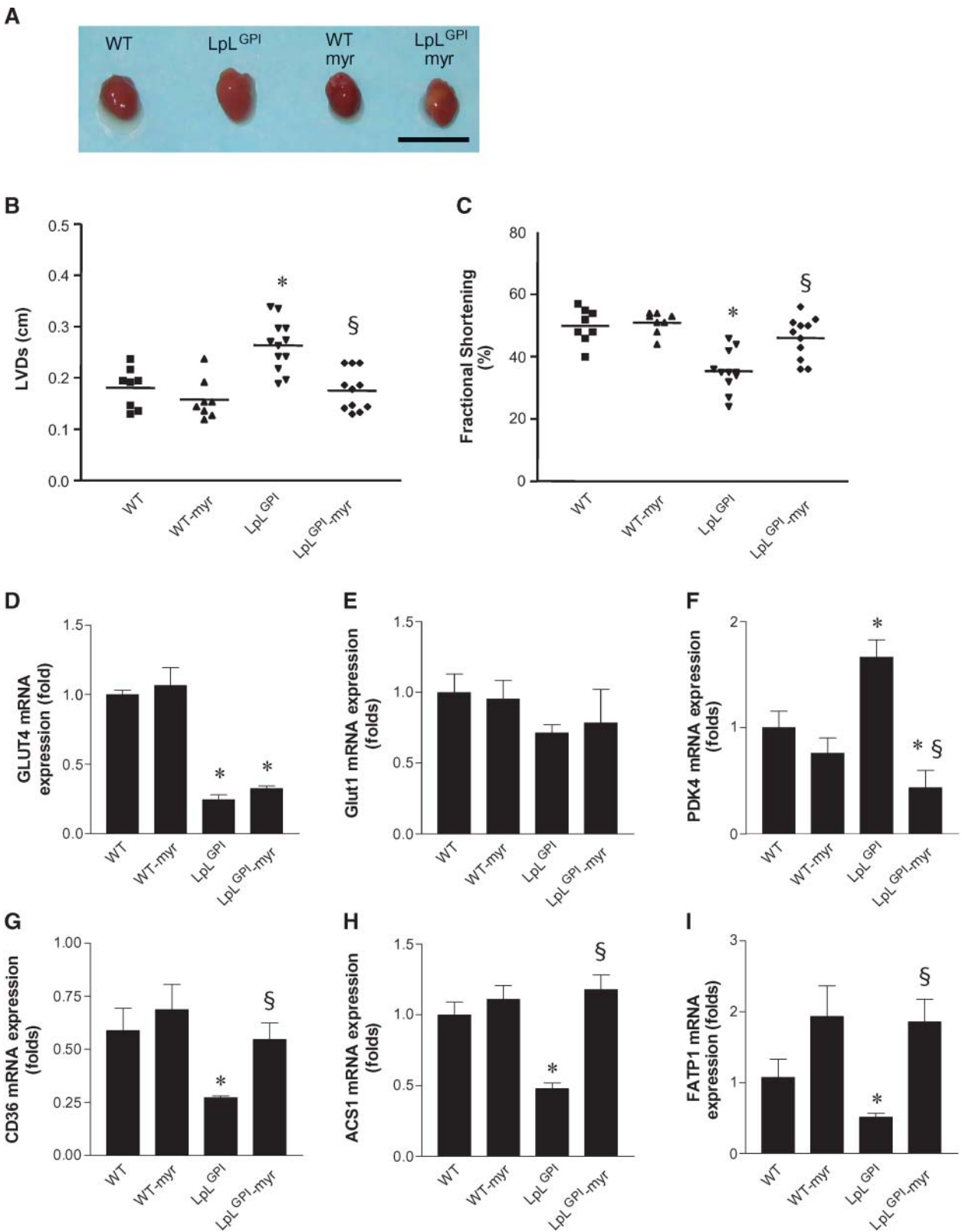
Fig. 1. Prevention of cardiomyopathy by myriocin in glycosylphosphotidylinositol (GPI)-anchored human lipoprotein lipase (LpL^{GPI}) hearts and regulation of cardiac gene expression in LpL^{GPI} mice. Eight week-old wild-type (WT) and LpL^{GPI} mice were fed chow or chow with 0.3 mg myriocin/kg/day for 6 weeks. Hearts from mice are shown (A). Chow-fed LpL^{GPI} mouse hearts were enlarged, but hearts from LpL^{GPI} mice fed myriocin-mixed chow were normal size. Left ventricular systolic diameter (LVD) (B) of the heart and fractional shortening (C) were measured by echocardiography as described in Materials and Methods (n = 8–12 each group). mRNA expression in the heart was measured by RT-PCR as described in Materials and Methods. Glucose-metabolizing genes GLUT4 (D), GLUT1 (E), and PDK4 (F). FA transporters CD36 (G), ACS1 (H), and FATP1 (I). Bar indicates 1 cm. *$P < 0.05$ versus WT; $^{§}P < 0.05$ versus LpL^{GPI}.
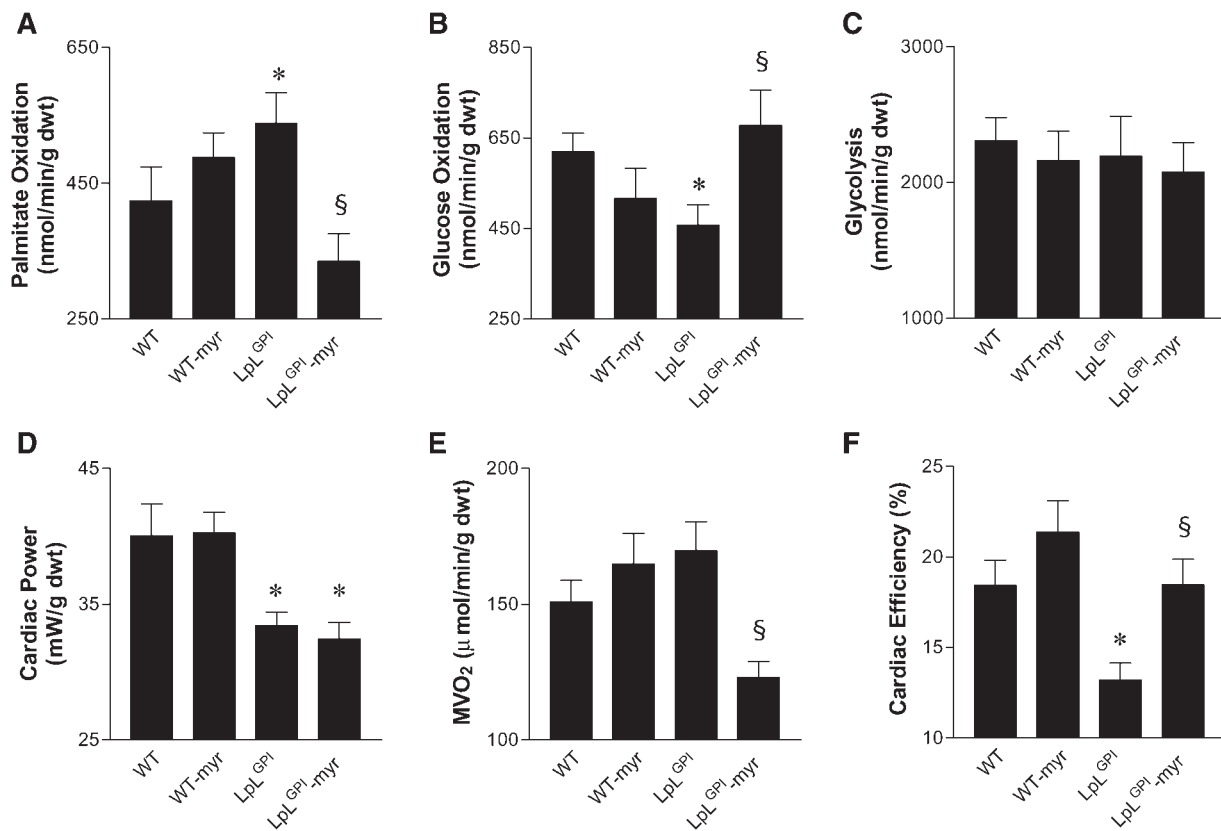
Fig. 2. Cardiac metabolism in isolated working hearts. Cardiac metabolism was measured in hearts isolated from 14 to 16 week-old male WT and LpL^{GPI} mice in the presence or absence of myriocin (n = 5 per genotype). All hearts were prepared and perfused in the working mode. Palmitate oxidation (A) was determined in separate perfused hearts by measuring the amount of ^3H_2O released from [9,10-^{3}H]palmitate. Glucose oxidation (B) was determined by trapping and measuring $^{14}CO_2$ released by the metabolism of [^{14}C]glucose, and glycolysis (C) was determined by measuring the amount of ^3H_2O released from the metabolism of exogenous [5-^{3}H]glucose. Cardiac power (D) was measured in hearts in which palmitate and glucose oxidation rates were determined (n = 5 each group). MVO$_2$ (E) and cardiac efficiency (F) were measured during palmitate oxidation. *$P < 0.05$ versus WT; $^\S P < 0.05$ versus LpL^{GPI}.

WT versus LpL^{GPI} mice at this age (14–16 weeks; see supplementary Fig. II). Thus, lipid-induced apoptosis is not the major factor contributing to cardiac dysfunction at this age. As described previously, LpL^{GPI} mice had early deaths from cardiac dysfunction (19). Myriocin treatment improved survival rates of LpL^{GPI} mice but did not restore survival rates to those of WT mice (**Fig. 5A**). We checked whether LpL^{GPI} mice might have tachyphylaxis to myriocin by measuring ceramide levels in 6 month-old mice. Cardiac ceramide was elevated even more, 66%, in 6 month-old LpL^{GPI} mice. As in the younger animals, the long-term myriocin treatment reduced the elevated ceramide in LpL^{GPI} hearts to WT levels (Fig. 5B), so tachyphylaxis to myriocin did not occur. These results suggest that although sphingolipid biosynthesis is one of the major factors contributing to the cardiac dysfunction observed in lipotoxic LpL^{GPI} mice, additional factors are likely to contribute as well.

Heterozygous deletion of SPT improves cardiac function of LpL^{GPI} mice

SPT is composed of two different subunits, LCB1 and LCB2. Heterozygous deletion of LCB1 or LCB2 results in reduced hepatic and plasma ceramide levels (32). To exclude nonspecific pharmacological effects of myriocin, we crossed LpL^{GPI} mice with whole-body heterozygous LCB1 knockout mice (LCB1$^{+/-}$/LpL^{GPI}). Hearts from 14 to 16 week-old LCB1$^{+/-}$/LpL^{GPI} mice demonstrated improved systolic function and fractional shortening when compared with LpL^{GPI} hearts (**Fig. 6A, B**). Cardiac ceramide levels in LCB1$^{+/-}$/LpL^{GPI} mice were decreased to the levels of WT mice (Fig. 6C). Heterozygous deletion of LCB1 downregulated LCB1 mRNA in the heart with intact LCB2 expression (Fig. 6D, E). Downregulation of LCB1 normalized elevated expression levels of ANF, BNP, and PDK4 in LpL^{GPI} hearts, but did not alter GLUT4 expression (Fig. 6F–I). Thus, reducing cardiac ceramide concentrations by heterozygous deletion of an SPT subunit also improved the lipotoxic cardiomyopathy of LpL^{GPI} transgenic mice.

DISCUSSION

Several lipids are likely to be toxic to tissues. We specifically explored whether ceramide, a lipid associated with cellular apoptosis, abnormal insulin signaling, and inflammation, mediated the lipotoxic phenotype in LpL^{GPI} mice. Our data show the following: *1*) SPT inhibition reduced
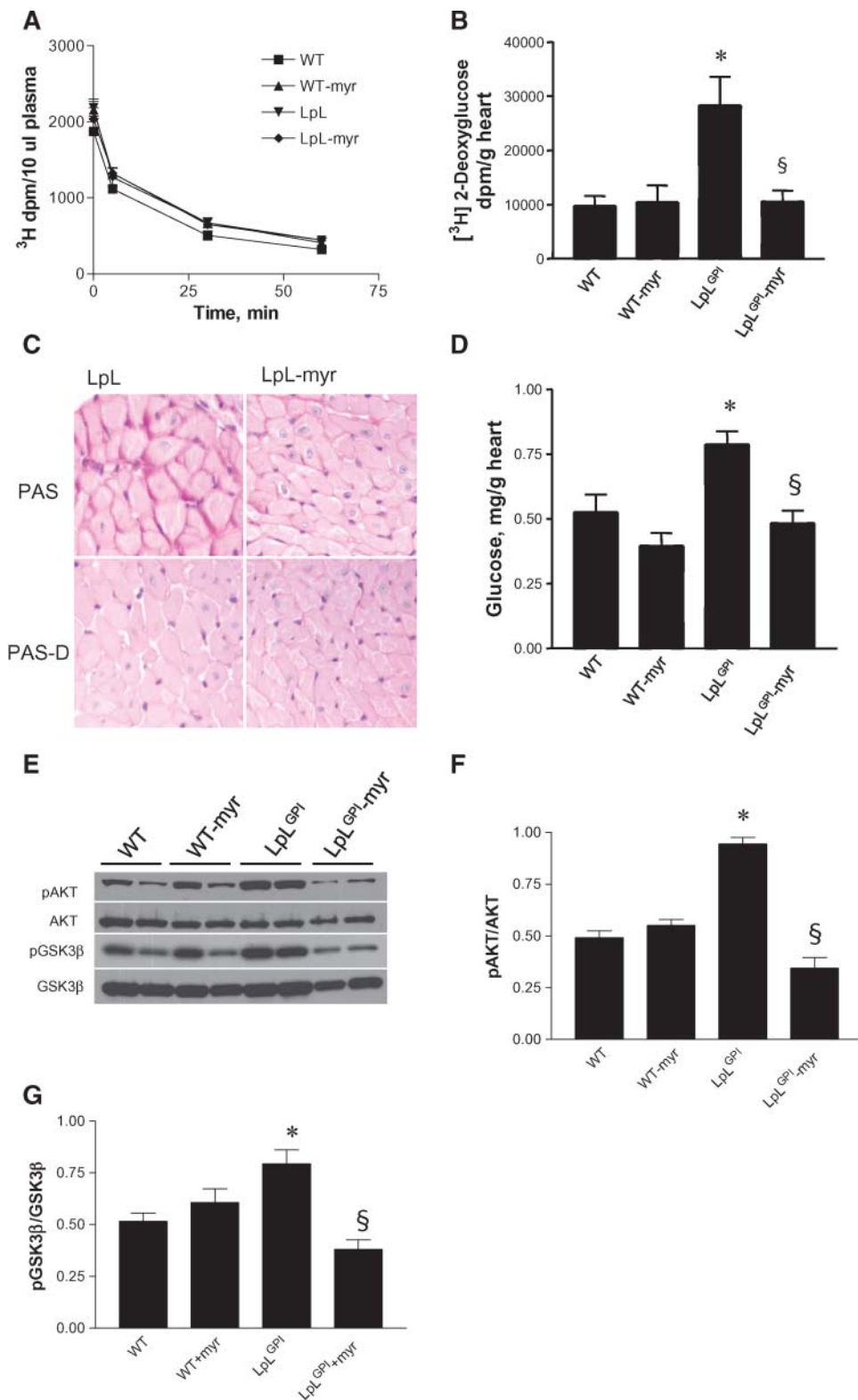
Fig. 3. Glucose uptake and glycogen accumulation. Basal glucose uptake was measured in hearts following an intravenous administration of 3 μCi of 2-deoxy-D-glucose (2-DG). Blood was collected 30 s and 5, 30, and 60 min following injection to determine plasma clearance (A) of 2-DG. At 60 min, hearts were perfused with PBS, tissues were excised, and radioactive counts were measured to calculate glucose uptake (n = 6–8 each group) (B). Cardiac glycogen in LpL^{GPI} heart was identified by periodic acid-Schiff (PAS) staining (C) of midventricular cross sections. Alternatively, the sections were treated with diastase to digest cardiac glycogen for comparison (PAS-D). Cardiac glycogen was measured biochemically as described in Materials and Methods (n = 10 each group); glucose released from glycogen hydrolysis is shown in D. PAKT and pGSK-3β in WT and LpL^{GPI} hearts were immunoblotted (E) and quantified by densitometry (F–G). *$P < 0.05$ versus WT; $^{§}P < 0.05$ versus LpL^{GPI}.
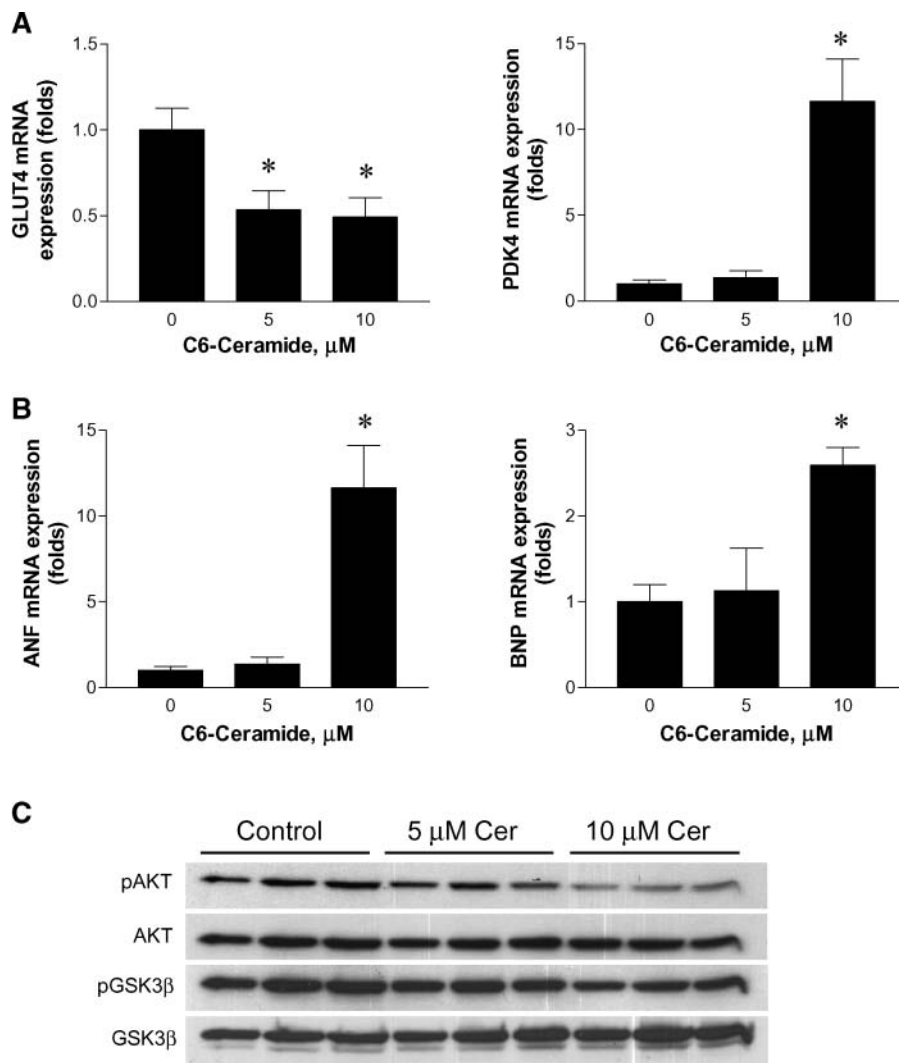
Fig. 4. Effects of ceramide in AC16 cells. AC16 cardiomyocytes were incubated with C6-ceramide at various concentrations for 16 h. mRNA expression of GLUT4 and PDK4 (A), and ANF and BNP (B) were analyzed by RT-PCR (n = 3). PAKT and pGSK-3β in AC16 cells were immunoblotted (C). *$P < 0.05$ versus no-treatment control.

ceramide content of LpL^{GPI} but not WT hearts; *2*) abnormal cardiac substrate utilization was corrected; *3*) this was associated with improved cardiac function; *4*) survival was improved; *5*) and a partial genetic deletion of SPT1 also was beneficial.

By selectively altering the ceramide biosynthetic pathway using pharmacologic and genetic methods, we showed that ceramide is a cardiac toxin in the LpL^{GPI} heart. Myriocin, a specific inhibitor of SPT, has been used to reduce ceramide levels in cancer cells (33), in models of atherosclerosis (34, 35), and insulin-resistant models (4). We tested whether myriocin decreased ceramide concentrations in WT and LpL^{GPI} mouse hearts. Plasma ceramide levels were reduced by this treatment. Although myriocin restored cardiac ceramide levels in LpL^{GPI} mice to WT levels, myriocin had no effect on levels in WT mice. This appears to be due to a compensatory activation of SPT in the WT mice, because gene expression of LCB1 and LCB2 was upregulated by myriocin treatment. LpL^{GPI} hearts had re-

duced SPT expression in the presence of increased tissue ceramide levels. This suggests that excess substrate availability increased cardiac ceramide synthesis. In contrast, myriocin treatment of WT mice did not alter hepatic SPT expression (34). Therefore, either liver ceramide content is unaltered by myriocin or cardiac and liver SPT regulation differ. Despite the lack of change in cardiac levels of cholesterol or FFA, myriocin-treated LpL^{GPI} mice had improved cardiac function. These data implicate ceramide as a basis for cardiac disease.

Lipid analysis of the LpL^{GPI} hearts demonstrated elevated cardiac DAG and ceramide. In contrast, long-chain fatty acyl CoA levels were decreased, probably due to increased cardiac FA oxidation. Reduced conversion of acyl CoAs into ceramide by SPT inhibition might cause increased cardiac acyl CoA pools. However, the SPT reaction utilizes saturated palmitoyl CoA specifically. The fact that not only saturated acyl CoAs but also short-chain and unsaturated acyl CoAs were reduced in LpL^{GPI} hearts (data not shown)
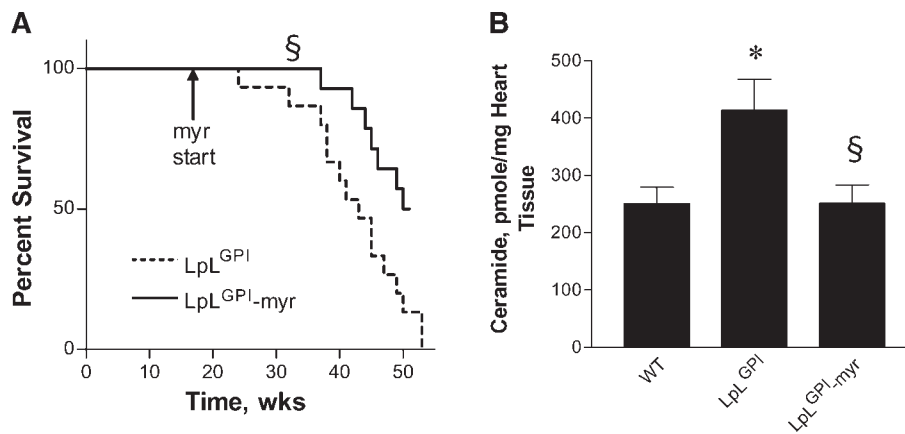
Fig. 5. Mortality rates and cardiac ceramide levels of LpL^{GPI} mice. LpL^{GPI} mice were fed control or myriocin-mixed chow (n = 14 each group) at the age of 12 weeks. Mortality of the mice was documented over the subsequent 40 weeks (A). Cardiac ceramide levels in 6 month-old mice were measured by liquid chromatography/tandem mass spectrometry (B) (n = 5 each group). *$P < 0.05$ versus WT; $^{§}P < 0.05$ versus LpL^{GPI}. The mortality of WT mice has been reported previously (19); >90% of these mice survive over 1 year.

suggests that these reductions were secondary to increased cardiac FA oxidation. LpL^{GPI} hearts oxidize more FAs and less glucose, and myriocin treatment reversed cardiac energy metabolism in isolated LpL^{GPI} hearts to that of WT. This was associated with no changes in the usual FA oxidation enzymes (CPT1 and ACO) and no changes in GLUT1 or GLUT4. PDK4, a PPAR-regulated gene that modulates glucose oxidation by allowing pyruvate to enter the tricarboxylic acid cycle, was increased in LpL^{GPI} hearts and reduced by myriocin. Thus, this gene was a better indicator of the metabolic changes found in the isolated perfused hearts. By studying the effects of ceramide on a cardiomyocyte-like cell line, we showed that ceramide alone increased PDK4 expression.

Unlike other organs, our data show that glucose uptake and oxidation are not directly correlated in the heart. Therefore, this mismatch of elevated glucose uptake and reduced oxidation in the LpL^{GPI} heart was because a large percent of cardiac glucose was shunted into glycogen rather than directly oxidized. At first we were surprised to find greater 2-DG uptake in the LpL^{GPI} hearts. However, we demonstrated that these hearts have more stored glycogen and that this was corrected by myriocin treatment. Whether increased glycogen stores were due to a direct effect of ceramide on glycogen synthesis pathways or were secondary to reduced cardiac function cannot be determined from our in vivo studies.

Glycogen synthesis is regulated by the AKT/GSK-3β pathway. Heart failure is associated with increased pGSK-3β, which might lead to increased glycogen synthesis. PAKT is increased in failing hearts of dogs and humans, and cardiac overexpression of AKT caused hypertrophy in mice (36–38). In contrast to studies in adipocytes (39) and skeletal muscle cells (40), we found no evidence that ceramide increases dephosphorylation of AKT via protein phosphatase 2A in lipotoxic hearts. In the failing heart, pAKT production is increased by non-insulin receptor-mediated pathways such as via G-protein-activated phosphatidylinositol 3-kinase γ (41–43). In AC16 cardiomyocytes, ceramide treatment

decreased pAKT and pGSK-3β, which is consistent with previous observations in skeletal muscle cells and adipocytes (39, 44, 45). Thus, increased pAKT and GSK-3β in lipotoxic hearts could be due to secondary effects of heart failure. However, the detailed mechanism of AKT/GSK-3β activation in the pathogenesis of cardiac failure is elusive and deserves further investigation.

Although myriocin-treated LpL^{GPI} mice had more-prolonged survival than untreated LpL^{GPI} mice, they still died earlier than did WT mice. Ceramide levels are greater in older mice. However, the myriocin treatment was equally effective in young and older mice. It is possible that the long-term effects of the treatment are suboptimal. Alternatively, additional processes leading to cardiac dysfunction are operative in the LpL^{GPI} mice. Thus, other bioactive lipids, such as DAG, which activates protein kinase C, could contribute to early death of lipid-driven cardiomyopathic mice (46, 47).

To exclude nonspecific pharmacological effects of myriocin, we crossed LpL^{GPI} transgenic mice with LCB1$^{+/-}$ mice that have reduced plasma and hepatic ceramide (32). Heterozygous deletion of the SPT subunit LCB1 normalized ceramide levels and PDK4 expression, improved cardiac function, and reduced the expression of heart failure markers. This pattern mirrors the effect of myriocin treatment on LpL^{GPI} hearts. Interestingly, expression of the cardiac failure markers ANF and BNP was downregulated by pharmacologic and genetic inhibition of SPT even further than those of WT. Thus, both pharmacological inhibition and genetic deletion of SPT improve these lipotoxic hearts. Whether ceramide inhibition will prove to be a common therapeutic modality to correct cardiomyopathy in other models of lipotoxicity requires further investigation.

Increased accumulation of cardiac lipids is associated with dilated cardiomyopathy, and this is true both for humans with obesity and diabetes (48–50) and in several animal models (5, 8, 51). One major issue is whether increased oxidation of lipids and generation of ROS or effects of toxic lipids are pathogenic. Although conversion of hearts
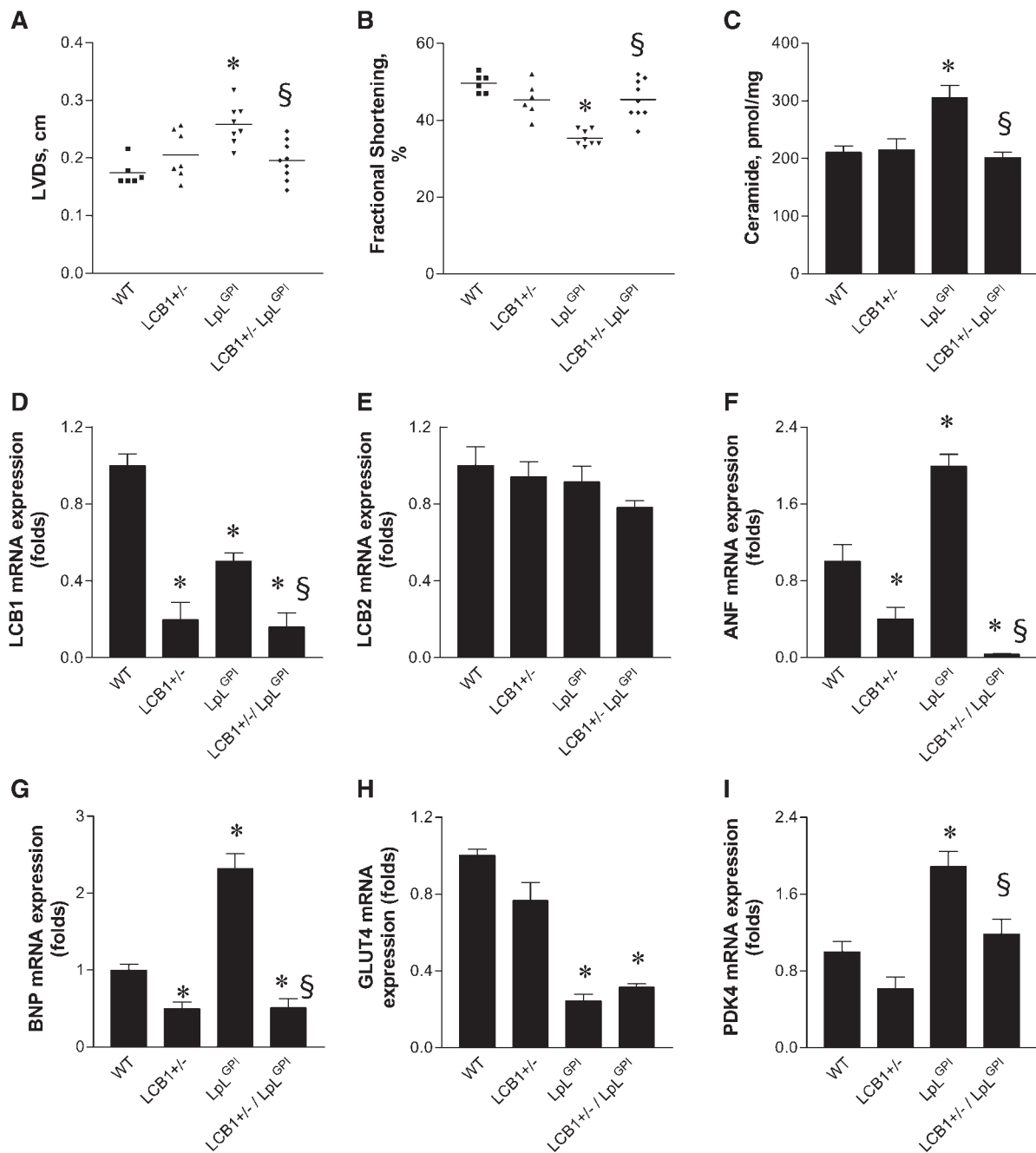
Fig. 6. Prevention of cardiomyopathy and regulation of cardiac gene expression by heterozygous deletion of LCB1 in LpL^{GPI} hearts. LVDs of the heart (A) and fractional shortening (B) in WT, heterozygous LCB1 knockout (LCB1$^{+/-}$), LpL^{GPI}, and LCB1$^{+/-}$/LpL^{GPI} mice (14–16 weeks old) were measured by echocardiography as described in Materials and Methods (n = 6–8 each group). Cardiac ceramide content (C) was measured by diacylglycerol kinase assay followed by TLC and autoradiography (n = 5 per genotype). Gene expression of LCB1 (D), LCB2 (E), ANF (F), BNP (G), GLUT4 (H) and PDK4 (I) was measured by real-time PCR and normalized by β-actin (n = 5 each group). *$P < 0.05$ versus WT; $^{§}P < 0.05$ versus LpL^{GPI}.

from use of FA to glucose as energy is beneficial in the setting of oxygen deficiency, i.e., ischemia, it is unclear whether disproportionate FA oxidation is harmful in other settings. It has been difficult to isolate the possible causes of lipotoxic cardiomyopathy, because genetic and pharmacologic interventions associated with increased FA oxidation also modulate lipid uptake and augment cardiomyocyte lipid accumulation. However, several genetic alterations have clearly linked lipid accumulation, rather than lipid oxidation, to cardiac dysfunction. Two genetic models of dilated cardiomyopathy, cardiac and muscle LpL overexpression on the PPARα knockout background (52) and cardiac-specific PPARδ knockout (53), are associated with reduced FA oxidation and cardiac lipid accumulation. Moreover, cardiomyopathy due to transgenic overexpression of PPARα is corrected by reduction of FA uptake by cross onto the CD36 knockout background, despite no reduction in FA oxidation (54). Thus, toxic lip-

ids, rather than excess FA oxidation, are likely to lead to heart dysfunction.

Excess lipid associated with dysfunctional tissues and organs is becoming a common problem in obesity. Islet cell, liver, and cardiac manifestations of lipotoxicity include type 2 diabetes, nonalcoholic steatohepatitis, and dilated cardiomyopathies. The underlying pathophysiology is likely to be similar in these three conditions. Other investigators have implicated ceramide as a toxic lipid (3, 4). By using a specific inhibitor of ceramide production and genetic methods, we provide evidence that this lipid is responsible, at least in part, for one form of dilated lipotoxic cardiomyopathy. The mechanisms behind myriocin's therapeutic benefit were examined and suggest that correction of defective cardiac energetics is involved. These studies provide a model for developing pharmacologic interventions for an increasingly important cause of human disease.▮▮▮

REFERENCES

1. Zhou, Y. T., P. Grayburn, A. Karim, M. Shimabukuro, M. Higa, D. Baetens, L. Orci, and R. H. Unger. 2000. Lipotoxic heart disease in obese rats: implications for human obesity. *Proc. Natl. Acad. Sci. USA.* **97:** 1784–1789.

2. Molavi, B., N. Rasouli, and P. A. Kern. 2006. The prevention and treatment of metabolic syndrome and high-risk obesity. *Curr. Opin. Cardiol.* **21:** 479–485.

3. Shimabukuro, M., M. Higa, Y. T. Zhou, M. Y. Wang, C. B. Newgard, and R. H. Unger. 1998. Lipoapoptosis in beta-cells of obese prediabetic fa/fa rats. Role of serine palmitoyltransferase overexpression. *J. Biol. Chem.* **273:** 32487–32490.

4. Holland, W. L., J. T. Brozinick, L. P. Wang, E. D. Hawkins, K. M. Sargent, Y. Liu, K. Narra, K. L. Hoehn, T. A. Knotts, A. Siesky, et al. 2007. Inhibition of ceramide synthesis ameliorates glucocorticoid-, saturated-fat-, and obesity-induced insulin resistance. *Cell Metab.* **5:** 167–179.

5. Chiu, H. C., A. Kovacs, D. A. Ford, F. F. Hsu, R. Garcia, P. Herrero, J. E. Saffitz, and J. E. Schaffer. 2001. A novel mouse model of lipotoxic cardiomyopathy. *J. Clin. Invest.* **107:** 813–822.

6. Finck, B. N., X. Han, M. Courtois, F. Aimond, J. M. Nerbonne, A. Kovacs, R. W. Gross, and D. P. Kelly. 2003. A critical role for PPAR-alpha-mediated lipotoxicity in the pathogenesis of diabetic cardiomyopathy: modulation by dietary fat content. *Proc. Natl. Acad. Sci. USA.* **100:** 1226–1231.

7. Son, N. H., T. S. Park, H. Yamashita, M. Yokoyama, L. A. Huggins, K. Okajima, S. Homma, M. J. Szabolcs, L. S. Huang, and I. J. Goldberg. 2007. Cardiomyocyte expression of PPARgamma leads to cardiac dysfunction in mice. *J. Clin. Invest.* **117:** 2791–2801.

8. Chiu, H. C., A. Kovacs, R. M. Blanton, X. Han, M. Courtois, C. J. Weinheimer, K. A. Yamada, S. Brunet, H. Xu, J. M. Nerbonne, et al. 2005. Transgenic expression of fatty acid transport protein 1 in the heart causes lipotoxic cardiomyopathy. *Circ. Res.* **96:** 225–233.

9. Hanada, K. 2003. Serine palmitoyltransferase, a key enzyme of sphingolipid metabolism. *Biochim. Biophys. Acta.* **1632:** 16–30.

10. Nilsson, A., and R. D. Duan. 2006. Absorption and lipoprotein transport of sphingomyelin. *J. Lipid Res.* **47:** 154–171.

11. Griffin, M. E., M. J. Marcucci, G. W. Cline, K. Bell, N. Barucci, D. Lee, L. J. Goodyear, E. W. Kraegen, M. F. White, and G. I. Shulman. 1999. Free fatty acid-induced insulin resistance is associated with activation of protein kinase C theta and alterations in the insulin signaling cascade. *Diabetes.* **48:** 1270–1274.

12. Xia, P., T. Inoguchi, T. S. Kern, R. L. Engerman, P. J. Oates, and G. L. King. 1994. Characterization of the mechanism for the chronic activation of diacylglycerol-protein kinase C pathway in diabetes and hypergalactosemia. *Diabetes.* **43:** 1122–1129.

13. Avignon, A., K. Yamada, X. Zhou, B. Spencer, O. Cardona, S. Saba-Siddique, L. Galloway, M. L. Standaert, and R. V. Farese. 1996. Chronic activation of protein kinase C in soleus muscles and other tissues of insulin-resistant type II diabetic Goto-Kakizaki (GK), obese/aged, and obese/Zucker rats. A mechanism for inhibiting glycogen synthesis. *Diabetes.* **45:** 1396–1404.

14. Listenberger, L. L., X. Han, S. E. Lewis, S. Cases, R. V. Farese, Jr., D. S. Ory, and J. E. Schaffer. 2003. Triglyceride accumulation protects against fatty acid-induced lipotoxicity. *Proc. Natl. Acad. Sci. USA.* **100:** 3077–3082.

15. Guo, W., S. Wong, W. Xie, T. Lei, and Z. Luo. 2007. Palmitate modulates intracellular signaling, induces endoplasmic reticulum stress, and causes apoptosis in mouse 3T3-L1 and rat primary preadipocytes. *Am. J. Physiol. Endocrinol. Metab.* **293:** E576–E586.

16. Wei, Y., D. Wang, F. Topczewski, and M. J. Pagliassotti. 2006. Saturated fatty acids induce endoplasmic reticulum stress and apoptosis independently of ceramide in liver cells. *Am. J. Physiol. Endocrinol. Metab.* **291:** E275–E281.

17. Borradaile, N. M., K. K. Buhman, L. L. Listenberger, C. J. Magee, E. T. Morimoto, D. S. Ory, and J. E. Schaffer. 2006. A critical role for eukaryotic elongation factor 1A-1 in lipotoxic cell death. *Mol. Biol. Cell.* **17:** 770–778.

18. Shi, H., M. V. Kokoeva, K. Inouye, I. Tzameli, H. Yin, and J. S. Flier. 2006. TLR4 links innate immunity and fatty acid-induced insulin resistance. *J. Clin. Invest.* **116:** 3015–3025.

19. Yagyu, H., G. Chen, M. Yokoyama, K. Hirata, A. Augustus, Y. Kako, T. Seo, Y. Hu, E. P. Lutz, M. Merkel, et al. 2003. Lipoprotein lipase (LpL) on the surface of cardiomyocytes increases lipid uptake and produces a cardiomyopathy. *J. Clin. Invest.* **111:** 419–426.

20. Davidson, M. M., C. Nesti, L. Palenzuela, W. F. Walker, E. Hernandez, L. Protas, M. Hirano, and N. D. Isaac. 2005. Novel cell lines derived from adult human ventricular cardiomyocytes. *J. Mol. Cell. Cardiol.* **39:** 133–147.

21. Belke, D. D., T. S. Larsen, E. M. Gibbs, and D. L. Severson. 2000. Altered metabolism causes cardiac dysfunction in perfused hearts from diabetic (db/db) mice. *Am. J. Physiol. Endocrinol. Metab.* **279:** E1104–E1113.

22. Belke, D. D., T. S. Larsen, E. M. Gibbs, and D. L. Severson. 2001. Glucose metabolism in perfused mouse hearts overexpressing human GLUT-4 glucose transporter. *Am. J. Physiol. Endocrinol. Metab.* **280:** E420–E427.

23. Belke, D. D., T. S. Larsen, G. D. Lopaschuk, and D. L. Severson. 1999. Glucose and fatty acid metabolism in the isolated working mouse heart. *Am. J. Physiol.* **277:** R1210–R1217.

24. Mazumder, P. K., B. T. O'Neill, M. W. Roberts, J. Buchanan, U. J. Yun, R. C. Cooksey, S. Boudina, and E. D. Abel. 2004. Impaired cardiac efficiency and increased fatty acid oxidation in insulin-resistant ob/ob mouse hearts. *Diabetes.* **53:** 2366–2374.

25. Folch, J., M. Lees, and G. H. Sloane Stanley. 1957. A simple method for the isolation and purification of total lipides from animal tissues. *J. Biol. Chem.* **226:** 497–509.

26. Hojjati, M. R., and X. C. Jiang. 2006. Rapid, specific, and sensitive measurements of plasma sphingomyelin and phosphatidylcholine. *J. Lipid Res.* **47:** 673–676.

27. Perry, D. K., A. Bielawska, and Y. A. Hannun. 2000. Quantitative determination of ceramide using diglyceride kinase. *Methods Enzymol.* **312:** 22–31.

28. Takuma, S., K. Suehiro, C. Cardinale, T. Hozumi, H. Yano, J. Shimizu, S. Mullis-Jansson, R. Sciacca, J. Wang, D. Burkhoff, et al. 2001. Anesthetic inhibition in ischemic and nonischemic murine heart: comparison with conscious echocardiographic approach. *Am. J. Physiol. Heart Circ. Physiol.* **280:** H2364–H2370.

29. Wang, C. Y., S. P. Mazer, K. Minamoto, S. Takuma, S. Homma, M. Yellin, L. Chess, A. Fard, S. L. Kalled, M. C. Oz, et al. 2002. Suppression of murine cardiac allograft arteriopathy by long-term blockade of CD40-CD154 interactions. *Circulation.* **105:** 1609–1614.

30. Yoshimura, A., Y. Toyoda, T. Murakami, H. Yoshizato, Y. Ando, and N. Fujitsuka. 2005. Glycogen depletion in intrafusal fibres in rats during short-duration high-intensity treadmill running. *Acta Physiol. Scand.* **185:** 41–50.

31. Ranalletta, M., H. Jiang, J. Li, T. S. Tsao, A. E. Stenbit, M. Yokoyama, E. B. Katz, and M. J. Charron. 2005. Altered hepatic and muscle substrate utilization provoked by GLUT4 ablation. *Diabetes.* **54:** 935–943.

32. Hojjati, M. R., Z. Li, and X. C. Jiang. 2005. Serine palmitoyl-CoA transferase (SPT) deficiency and sphingolipid levels in mice. *Biochim. Biophys. Acta.* **1737:** 44–51.

33. Chalfant, C. E., K. Rathman, R. L. Pinkerman, R. E. Wood, L. M. Obeid, B. Ogretmen, and Y. A. Hannun. 2002. De novo ceramide regulates the alternative splicing of caspase 9 and Bcl-x in A549 lung adenocarcinoma cells. Dependence on protein phosphatase-1. *J. Biol. Chem.* **277:** 12587–12595.

34. Park, T. S., R. L. Panek, S. B. Mueller, J. C. Hanselman, W. S. Rosebury, A. W. Robertson, E. K. Kindt, R. Homan, S. K. Karathanasis, and M. D. Rekhter. 2004. Inhibition of sphingomyelin synthesis reduces atherogenesis in apolipoprotein E-knockout mice. *Circulation.* **110:** 3465–3471.

35. Hojjati, M. R., Z. Li, H. Zhou, S. Tang, C. Huan, E. Ooi, S. Lu, and X. C. Jiang. 2005. Effect of myriocin on plasma sphingolipid metabolism and atherosclerosis in apoE-deficient mice. *J. Biol. Chem.* **280:** 10284–10289.

36. Haq, S., G. Choukroun, H. Lim, K. M. Tymitz, F. del Monte, J. Gwathmey, L. Grazette, A. Michael, R. Hajjar, T. Force, et al. 2001. Differential activation of signal transduction pathways in human hearts with hypertrophy versus advanced heart failure. *Circulation.* **103:** 670–677.

37. Ananthakrishnan, R., G. W. Moe, M. J. Goldenthal, and J. Marin-Garcia. 2005. Akt signaling pathway in pacing-induced heart failure. *Mol. Cell. Biochem.* **268:** 103–110.

38. Shiojima, I., K. Sato, Y. Izumiya, S. Schiekofer, M. Ito, R. Liao, W. S. Colucci, and K. Walsh. 2005. Disruption of coordinated cardiac hypertrophy and angiogenesis contributes to the transition to heart failure. *J. Clin. Invest.* **115:** 2108–2118.

39. Stratford, S., K. L. Hoehn, F. Liu, and S. A. Summers. 2004. Regulation of insulin action by ceramide: dual mechanisms linking ceramide accumulation to the inhibition of Akt/protein kinase B. *J. Biol. Chem.* **279:** 36608–36615.

40. Chavez, J. A., and S. A. Summers. 2003. Characterizing the effects of saturated fatty acids on insulin signaling and ceramide and diacylglycerol accumulation in 3T3-L1 adipocytes and C2C12 myotubes. *Arch. Biochem. Biophys.* **419:** 101–109.

41. DeBosch, B., I. Treskov, T. S. Lupu, C. Weinheimer, A. Kovacs, M. Courtois, and A. J. Muslin. 2006. Akt1 is required for physiological cardiac growth. *Circulation.* **113:** 2097–2104.

42. Nienaber, J. J., H. Tachibana, S. V. Naga Prasad, G. Esposito, D. Wu, L. Mao, and H. A. Rockman. 2003. Inhibition of receptor-localized PI3K preserves cardiac beta-adrenergic receptor function and ameliorates pressure overload heart failure. *J. Clin. Invest.* **112:** 1067–1079.

43. Oudit, G. Y., Z. Kassiri, M. P. Patel, M. Chappell, J. Butany, P. H. Backx, R. G. Tsushima, J. W. Scholey, R. Khokha, and J. M. Penninger. 2007. Angiotensin II-mediated oxidative stress and inflammation mediate the age-dependent cardiomyopathy in ACE2 null mice. *Cardiovasc. Res.* **75:** 29–39.

44. Chavez, J. A., T. A. Knotts, L. P. Wang, G. Li, R. T. Dobrowsky, G. L. Florant, and S. A. Summers. 2003. A role for ceramide, but not diacylglycerol, in the antagonism of insulin signal transduction by saturated fatty acids. *J. Biol. Chem.* **278:** 10297–10303.

45. Summers, S. A., L. A. Garza, H. Zhou, and M. J. Birnbaum. 1998. Regulation of insulin-stimulated glucose transporter GLUT4 translocation and Akt kinase activity by ceramide. *Mol. Cell. Biol.* **18:** 5457–5464.

46. Listenberger, L. L., and J. E. Schaffer. 2002. Mechanisms of lipoapoptosis: implications for human heart disease. *Trends Cardiovasc. Med.* **12:** 134–138.

47. Carlsson, C., L. A. Borg, and N. Welsh. 1999. Sodium palmitate induces partial mitochondrial uncoupling and reactive oxygen species in rat pancreatic islets in vitro. *Endocrinology.* **140:** 3422–3428.

48. Sharma, S., J. V. Adrogue, L. Golfman, I. Uray, J. Lemm, K. Youker, G. P. Noon, O. H. Frazier, and H. Taegtmeyer. 2004. Intramyocardial lipid accumulation in the failing human heart resembles the lipotoxic rat heart. *FASEB J.* **18:** 1692–1700.

49. Peterson, L. R., P. Herrero, K. B. Schechtman, S. B. Racette, A. D. Waggoner, Z. Kisrieva-Ware, C. Dence, S. Klein, J. Marsala, T. Meyer, et al. 2004. Effect of obesity and insulin resistance on myocardial substrate metabolism and efficiency in young women. *Circulation.* **109:** 2191–2196.

50. McGavock, J. M., I. Lingvay, I. Zib, T. Tillery, N. Salas, R. Unger, B. D. Levine, P. Raskin, R. G. Victor, and L. S. Szczepaniak. 2007. Cardiac steatosis in diabetes mellitus: a 1H-magnetic resonance spectroscopy study. *Circulation.* **116:** 1170–1175.

51. Finck, B. N., J. J. Lehman, T. C. Leone, M. J. Welch, M. J. Bennett, A. Kovacs, X. Han, R. W. Gross, R. Kozak, G. D. Lopaschuk, et al. 2002. The cardiac phenotype induced by PPARalpha overexpression mimics that caused by diabetes mellitus. *J. Clin. Invest.* **109:** 121–130.

52. Nohammer, C., F. Brunner, G. Wolkart, P. B. Staber, E. Steyrer, F. J. Gonzalez, R. Zechner, and G. Hoefler. 2003. Myocardial dysfunction and male mortality in peroxisome proliferator-activated receptor alpha knockout mice overexpressing lipoprotein lipase in muscle. *Lab. Invest.* **83:** 259–269.

53. Cheng, L., G. Ding, Q. Qin, Y. Huang, W. Lewis, N. He, R. M. Evans, M. D. Schneider, F. A. Brako, Y. Xiao, et al. 2004. Cardiomyocyte-restricted peroxisome proliferator-activated receptor-delta deletion perturbs myocardial fatty acid oxidation and leads to cardiomyopathy. *Nat. Med.* **10:** 1245–1250.

54. Yang, J., N. Sambandam, X. Han, R. W. Gross, M. Courtois, A. Kovacs, M. Febbraio, B. N. Finck, and D. P. Kelly. 2007. CD36 deficiency rescues lipotoxic cardiomyopathy. *Circ. Res.* **100:** 1208–1217.